The Role of LS-DYNA® in the Design of the New London Electric Taxi

Simon Hart[1], Jamie Dennis[1], Gavin Newlands[1]

[1]Arup (Advanced Technology and Research), Solihull UK

1 Abstract

The iconic London taxi is known worldwide. The London Taxi Company (LTC) has produced this much loved vehicle for many years with few radical changes. Recently, zero-emission legislation in London and the global demand for cleaner vehicles has prompted an evolution in its design. With investment from owner Geely, the newly branded London EV Company (LEVC) will produce several thousand electric taxis per year from its new headquarters in Coventry, UK. The designers, Emerald Automotive Design (EAD), engaged Arup to analyse all structural and safety load cases. This paper discusses how the versatility of LS-DYNA and the modularity of the keyword file enabled Arup to use a single-model approach for all analysis - from full vehicle crashworthiness through to component-level durability checks - and how this facilitated an efficient division of activity between remote teams in the UK and China. The application of both explicit and implicit LS-DYNA to the various load cases is considered, together with the correlation against physical testing. Special challenges were posed by the requirement to comply with Transport for London's (TfL) Conditions of Fitness and the need to protect the high-voltage components. Reliance on the LS-DYNA predictions was high, with few prototype stages afforded by the accelerated programme. Successful progression directly from simulation to legislative testing sign-off was achieved for cases including pedestrian protection. Arup's use of LS-DYNA was key in bringing this lightweight bonded aluminium taxi to market, whilst minimising energy consumption and delivering a solution to the issue of sustainable city transport.

2 Introduction

The black cab has long been synonymous with travel in central London. The first horse-drawn hackney coaches began transporting passengers around the capital early in the 17th century. The cabs underwent a number of iterations in design over the following decades but remained muscle-powered until the introduction of the first motorised taxis just before the turn of the 20th century [1]. Perhaps surprisingly, these first motor cabs were electrically powered and nicknamed "hummingbirds" due to the distinctive noise they made. Introduced by the London Electrical Cab Company in 1897, approximately 80 of these three-horse-power vehicles covered more than 500,000 combined miles at a top speed of 9 mph before the company ceased operating in 1899 [2]. The first petrol taxis were introduced only a few years later and soon came to dominate the market, led by the Austin Motor Company and dealer Mann & Overton [1].

Following the end of World War Two, coachbuilder Carbodies won a contract to build bodies for the Austin FX3 taxi, released in 1948. This was followed by the production of the FX4 (Figure 1) in 1958 which, with its distinctive style, has come to be instantly recognisable as a London taxi. The long serving FX4 was produced until 1997, during which time the intellectual rights were transferred to Carbodies, who under new ownership by Manganese Bronze Holdings became London Taxis International (LTI), and the FX4 became the LTI Fairway [1].

Fig.1:   Austin FX4 [3].   Fig.1 - LTC TX4 ([4])

LTI introduced the TX1 in 1997, taking a number of styling cues from the FX4. This was followed by the updated TXII and TX4 (Fig.1) models in 2002 and 2007 respectively. The TX series established LTI as a worldwide supplier of London-type taxis. The company was rebranded as the London Taxi Company (LTC) in 2010 [5]. Chinese automaker Geely had been working with LTC since 2006 in a joint venture to manufacture taxis in Shanghai [6]. In 2013 Geely took over the remainder of LTC's assets after financial difficulties had forced it into administration [7], allowing production of the London black cab to resume in Coventry.

In January 2014, London's Mayor announced plans for new taxi licensing requirements as part of the drive to phase out traditional combustion driven taxis [8]. From 1 January 2018 no new diesel taxis will be granted a taxi vehicle license, and all newly registered taxis must be zero emissions capable (ZEC) with a minimum 30 mile zero emissions range [9]. London was not the only location striving for cleaner city transport, with centres around the world making similar commitments. Amsterdam, for example, laid plans to extend its low emissions zone to include taxis from the start of 2018, and have most traffic groups emissions-free by 2025 [10].

An evolution in taxi design was required. More than a century after they first appeared, London taxis with an electric powertrain would once again convey passengers to their destinations. The London Taxi Company began development of the TX Electric Taxi with Emerald Automotive Design (EAD) and, with its release at the beginning of 2018, became the London EV Company (LEVC).

Fig.3:   Company Hierarchy

3 The New Electric Taxi Project

The new TX Electric Taxi differs significantly from its predecessors. It is a Plug-in Hybrid Electric Vehicle (PHEV) for use in modern cities, with energy efficiency and low emissions as primary design objectives. Consequently, the vehicle must be lightweight to allow the electric drivetrain to work effectively. The body structure is predominantly aluminium, bonded using a hot-cure epoxy adhesive. Exterior body panels are manufactured from fibre reinforced plastic composite. The vehicle is driven from the rear by an electric motor, powered by a lithium-ion battery located under the floor structure with 31kWh capacity. The range of the vehicle in pure electric model is approximately 80 miles. A small petrol engine is located at the front of the vehicle and acts as a range-extender; charging the battery without the need to stop, increasing the total range to nearly 380 miles before refilling [11].

In addition to its new architecture and powertrain, the safety targets for the new taxi were set to the highest level. The vehicle is engineered to meet the strictest requirements of European consumer testing, which include protection for the vehicle's occupants in different crash scenarios, electronically assisted safety features and protection for vulnerable road users. This latter attribute is particularly relevant for a city vehicle.

Fig.4:   LEVC TX [5]

The TX Electric Taxi development programme was short, considering the design strategy was a radical departure from previous generations of the vehicle. Additionally, a new manufacturing facility would be constructed and commissioned in the same period, leading to an ambitious launch date in early 2018. Concept development was completed during 2014, with Attribute Prototypes (AP) available in late 2015. AP development and verification continued throughout 2016, leading to Verification Prototype (VP) availability in early 2017. VP testing was completed during 2017 and Pre-Production (PP) vehicles were signed off during legislative testing in late 2017. Start of production commenced in late 2017 and product launch was in January 2018.

The compressed nature of the programme called for integration of Computer Aided Engineering (CAE) from the earliest concept stages. Arup was chosen to provide all structural and safety related CAE, supporting development of Body-in-White (BIW), closures, interior and exterior systems, occupant and pedestrian safety, crashworthiness, Noise Vibration and Harshness (NVH), strength and durability. As prototype testing was limited, with only one phase of testing for AP and VP, reliable and accurate CAE predictions were required.

LS-DYNA was chosen as the sole analysis package for Arup's delivery towards the TX due to its ability to solve multiple solution types across a range of linear and non-linear problems, and the modularity of its keyword file structure. This enabled Arup to utilise a single-model approach to their work, with all of the required load-cases drawing from the same set of LS-DYNA include files, and all

being analysed in the same domain. The risk of information loss in time-consuming model conversions was eliminated, both implicit and explicit solutions could be analysed, and an efficient and consistent work flow could be maintained.

Arup's team was structured to support delivery of the TX with high value against a short programme. A team of up to 12 engineers working simultaneously, split equally between the UK and Shanghai, allowed Arup to take advantage of savings whilst being able to support Emerald and the design team directly with engineers sitting client-side in the design studio. The time difference allowed for handovers of urgent tasks at the end of one team's working day to the other at the start of theirs, and the significant automotive CAE experience and LS-DYNA supporting computing infrastructure in both regions could be utilised.

4 Crashworthiness Analysis

A significant proportion of CAE activity was supporting the structural design to meet crashworthiness targets. The main cases that were considered reflected the intended European market:

- 64 km/h Offset Deformable Barrier (ODB) frontal impact;
- 50 km/h Full Frontal Barrier (FFB);
- 32 km/h side pole impact;
- 50 km/h Moving Deformable Barrier (MDB) side impact;
- 50 km/h rear impact;
- Roof crush resistance;
- Low speed impacts for repairability.

Fig.5:   TX Finite Element Model

The use of a modularised model that utilised include files was key to quickly running the large number of iterations required to reach the optimal solution for each case. As design changes were implemented in response to one loadcase, they could be quickly assessed for other cases by substituting the relevant include files. This methodology also applied to the non-crash cases; the effect of changes made to improve crash performance could be quickly assessed for body stiffness in the same way. **Error! Reference source not found.** shows the TX crash finite element model.

Transport for London's (TfL) Conditions of Fitness [12] require taxis to be able to turn 180 degrees between two walls 28 ft apart. To accommodate the wheel envelopes, the TX's front longitudinal members are forced particularly close to each other, making the packaging strategy complex, especially with respect to crashworthiness. Arup drove a number of packaging changes using the results of crash simulations. **Error! Reference source not found.** shows an example of the level of agreement achieved between simulation and test, in this case for the B-Pillar acceleration during 64 km/h offset deformable barrier impact. **Error! Reference source not found.** and **Error! Reference source not found.** show examples of analytical predictions and the subsequent test images.
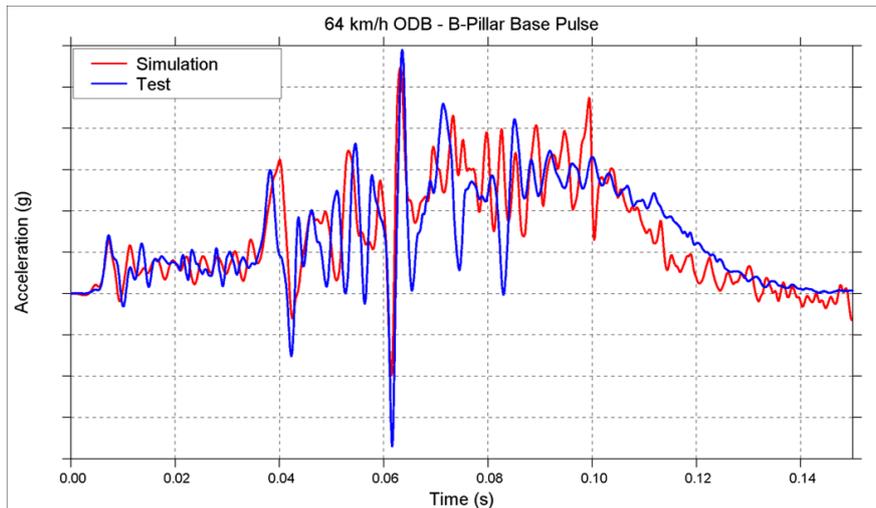
Fig.6:   *Example of Acceleration Time History Comparison for 64 km/h ODB Impact*

Fig.7:   *Comparison of Test and CAE; Rear Impact & Front Under-run*

The TX offers state of the art protection to its occupants. The driver is protected by collapsible steering column, front and side airbags, seatbelt pretensioners and load limiters. Curtain airbags protect driver and second and third row occupants. The driver's seat is designed to limit whiplash injuries. Forward facing seats in the passenger compartment feature anti-submarining devices and are fitted with 3-point seatbelts with load limiters, tuned to limit kinematics and chest compression in frontal impact. Child seat anchors are provided.
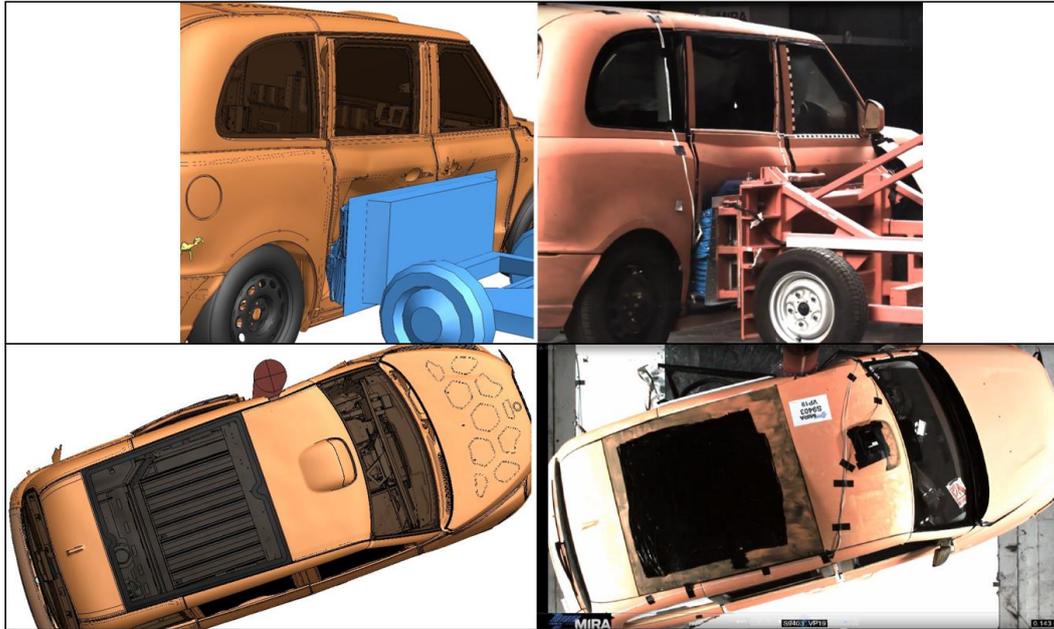
Fig.8:   Comparison of Test and CAE; Side Barrier Impact & Pole Impact

Due to the limited amount of prototype testing, calibration of the restraint system sensors relied heavily on CAE predictions of vehicle accelerations in impact events. The CAE model was used to predict vehicle accelerations in twenty-two different impact configurations, to provide sufficient data for sensor calibration prior to VP testing. Remote firing of the restraint systems was employed in the VP tests until validation of the calibration was complete. Live firing was used in the final sign off tests with PP vehicles. **Error! Reference source not found.** shows an example of a front impact simulation with occupant and restraint system modelled, in this case the 50 km/h flat frontal barrier impact.

Fig.9:   Front Impact with Small Female ATD, CAE & Test

A Conditions of Fitness compliant taxi must provide access to passengers in wheelchairs. The TX is fitted with an integral ramp, stowed under the rear floor. Passengers in wheelchairs can face forwards in the vehicle and additional restraints are provided for both the passenger and wheelchair in this position. For passengers in the rearward facing foldaway seats, three-point seatbelts are anchored to the structural divider that separates the driver compartment. Figure 9 shows images of the CAE models used to for occupant safety development during the programme.
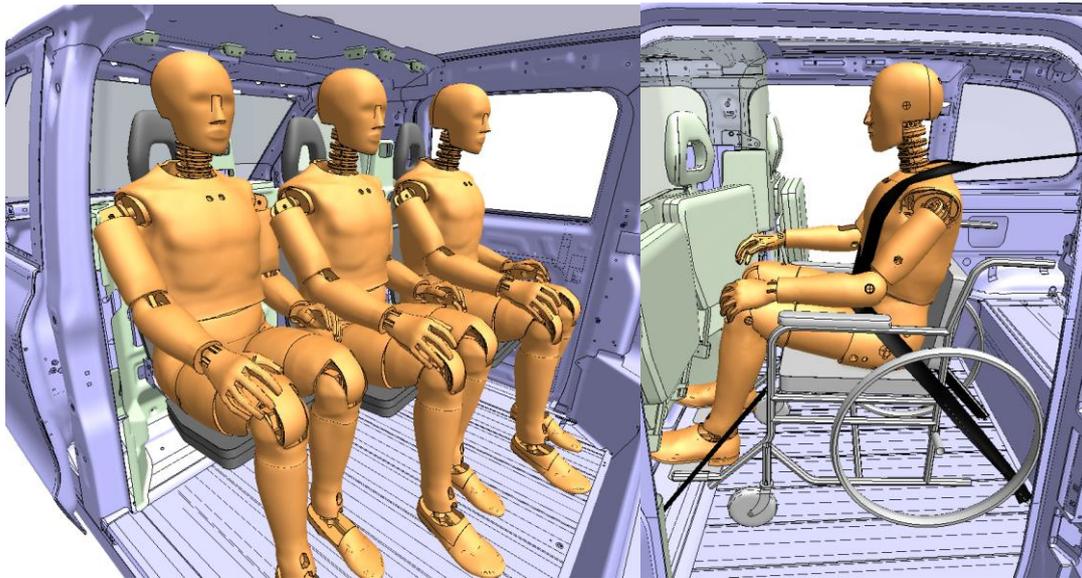
Fig.10:   Second Row Occupant Model, Fig.11 Model of Occupant in Wheelchair

A key aspect of the crashworthiness analysis was the ability to predict strength of the bonded joints in the aluminium body structure (**Error! Reference source not found.**) during a crash event. An epoxy adhesive is applied to BIW joints during assembly and the whole body is cured in an oven during a single cycle. Mechanical fasteners (rivets) are present in the joints to retain parts prior to curing and to add strength in critical locations. The adhesive was represented using solid elements in the CAE model.   The solid elements are projected between adjacent parts in the BIW and are mesh independent; a tied contact surface is used to constrain the solid element nodes to the structural parts, which are usually meshed in shell elements.

Material model 169 (ARUP_ADHESIVE) [13] was chosen to model the epoxy adhesive. This material model has non volume conserving plasticity and is available for solid element formulations 1, 2 and 15. Node numbering of the solid elements was used to identify the thickness direction of the bond between surfaces 1-2-3-4 to 5-6-7-8 using parameter THKDIR, as illustrated in Fig.2. The use of an automatic adhesive mesh generator, such as the connection manager in Oasys PRIMER [14] will ensure that the node numbering is consistent. In the usual case of substrates modelled with shell elements lying on the mid-surface, the solid element bond thickness will be thicker than reality. This is accounted for with the parameter BTHK, which can be set to the actual bond thickness, typically less than 1.0mm.
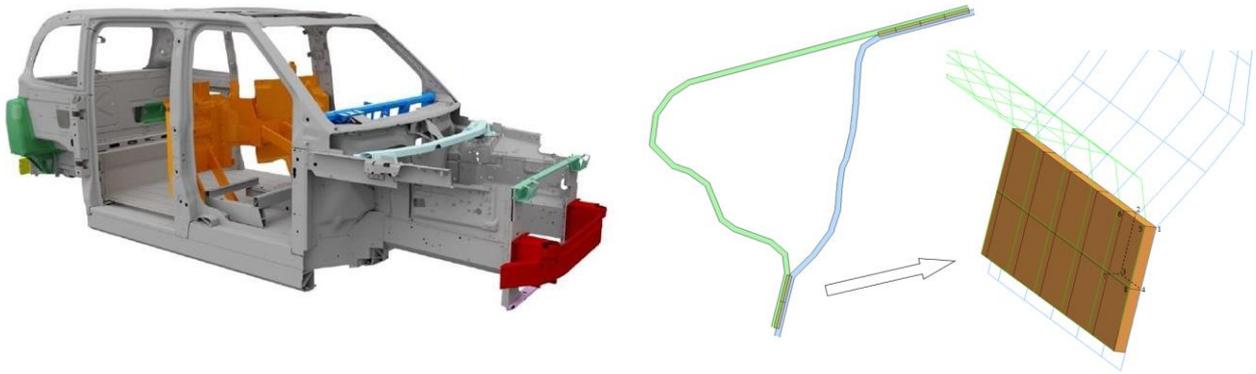
Fig.12:   TX Bonded Aluminium BIW, Fig.2 - Detail of Solid Elements used for Adhesive

The yield surface for material 169 is defined as a power-law combination of tensile and shear strengths, which are typically provided on manufacturers' datasheets. Fracture energy is defined with parameters GCTEN and GCSHR, from which the traction-separation curves are internally derived for tension and shear respectively. Early validation of the material model was completed using tensile test coupons used to verify correct function of the curing oven. During AP phase the material parameters were improved using crash test results from the AP vehicles. With this limited dataset, it was possible to achieve satisfactory agreement with test results and more importantly establish a reliable predictive model for the VP development phase.

5 Structural Strength, Stiffness and NVH

Structural strength, stiffness and NVH are discussed together in this section, as they are often considered together as linear cases and analysed with a different solver. During the TX programme LS-DYNA was used as the primary solver and therefore these cases were analysed using the LS-DYNA implicit solver. This had the following advantages:

- One model could be maintained without the need to translate into different formats;
- Modifications made during stiffness analysis could easily be assessed in the crash models and vice-versa;
- Non-linear static analysis could be activated if required, e.g. to consider the effect of contact, material non-linearity, large displacements, etc.

For BIW stiffness analysis, the common BIW include file also used for crashworthiness analysis was analysed. Therefore, assembly of the stiffness model was simply a case of selecting the appropriate include files (BIW, material definitions, implicit solver control cards and restraints). **Error! Reference source not found.** illustrates the method and shows a typical torsional stiffness result. Torsional and bending stiffness of the BIW were evaluated; **Error! Reference source not found.** shows the comparison between the analytical prediction and AP test result.
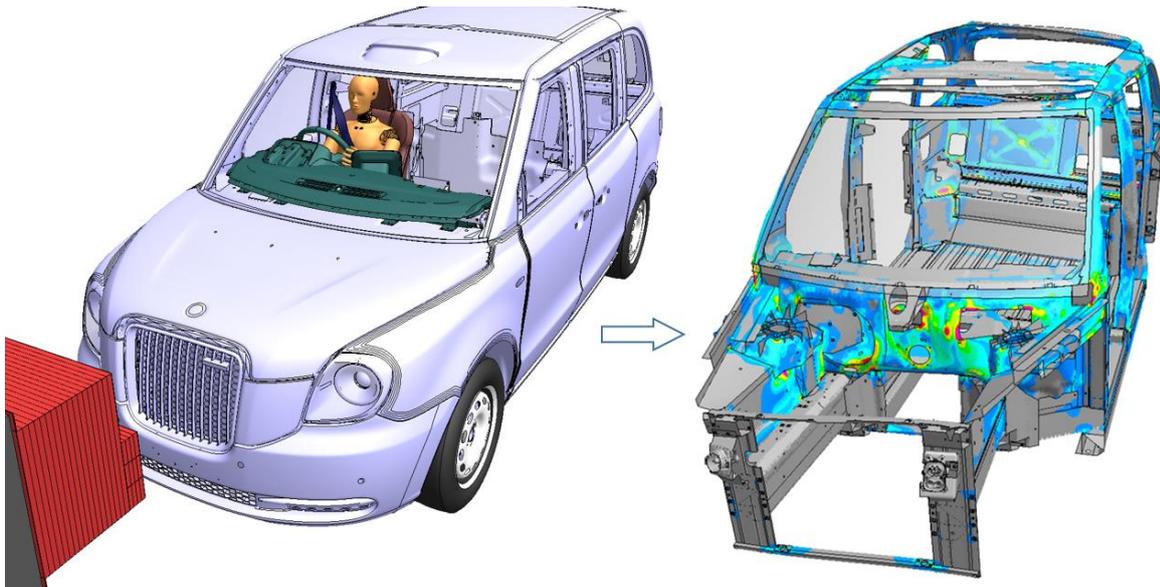
Fig.14:   Modular Model Approach and Typical Stiffness Analysis Output

The scope of the NVH assessment was limited to low frequency structure borne phenomena, commensurate with the structural finite element model used in the development programme. The main tools for assessing NVH and vehicle refinement were modal analysis and frequency response analysis. Normal modes were computed for BIW, closures, interior and exterior systems separately and at trimmed body level. In LS-DYNA, modal analysis is activated with the addition of the CONTROL_IMPLICIT_EIGENVALUE card and requesting implicit analysis with IMFLAG on CONTROL_IMPLICIT_GENERAL. To aid understanding of structural performance, modal stresses were requested using MSTRES on CONTROL_IMPLICIT_EIGENVALUE [15].
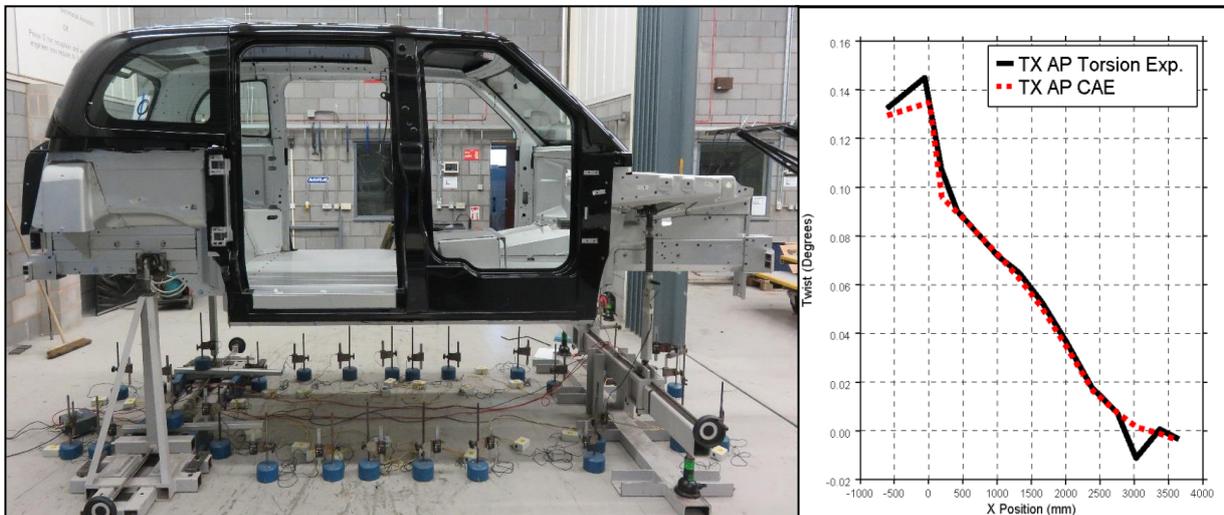

Fig.15:   BIW Static Torsion Test and Comparison with CAE

The range extender in the TX operates at a set number of discrete speeds to charge the on-board battery. In a series-hybrid vehicle, the engine does not directly drive the wheels nor does it idle or continuously vary its speed under the control of the driver. Therefore, target modal frequencies were placed around these known running speeds. The engine is turbo charged with three cylinders, of capacity 1.5 litres [11]. Therefore, the dominant orders considered were 1.0, 1.5 and 3.0 multiples of engine speed. Primary structural modes, panel modes, modes of interior systems such as steering wheel, instrument panel and driver-passenger dividing screen were evaluated and compared to targets. Where necessary the CAE model was used to guide design changes to meet targets, for example the supporting strategy for the roof panel, which is a large composite part.
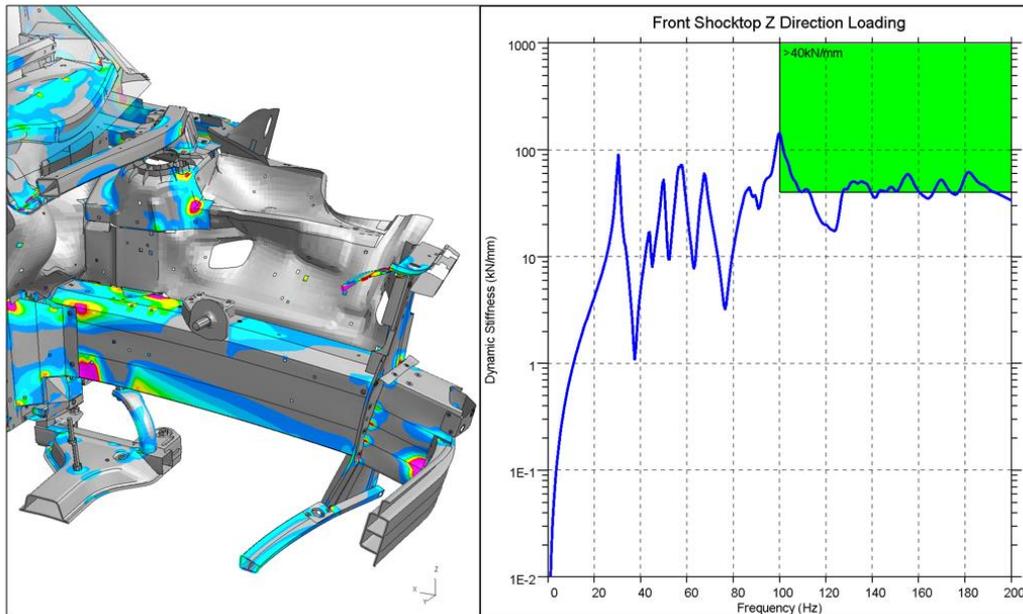
Fig.16:   Dynamic Stiffness of Front Suspension Mount

Frequency response analysis was completed at BIW level to evaluate dynamic stiffness of the subsystem mounting points up to 200Hz. In LS-DYNA this is achieved by calculating the forced response of the system in the frequency domain using modal superposition. The approximate dynamic response of the system is computed at a given frequency as a summation of responses from all calculated mode shapes. This calculation is repeated for all frequencies of interest to produce a response spectrum, in this case displacement per unit force vs. frequency. The frequency response function (FRF) gives an insight into how the structure responds at different forcing frequencies and can be used to compare the dynamic stiffness of the mounting point against the target value. **Error! Reference source not found.** shows a stiffness FRF for the front suspension mount, comparing the predicted response against the target value. The figure shows the forced response at 123Hz, which influences the stiffness at that frequency.

LS-DYNA input is an extension of the modal analysis discussed above. Modes for consideration in the frequency response calculation are selected via the CONTROL_IMPLICIT_EIGENVALUE card. In this case, modes up to 400Hz were calculated to evaluate dynamic stiffness in the range 0-200Hz. The card FREQUENCY_DOMAIN_FRF was used to define the forced response. On this card the excited degree of freedom and the response degree of freedom are identified together with the type of excitation (force or enforced motion). Several options for damping are available; in this case a small amount of modal damping was used (DAMPF).

The LS-DYNA implicit solver was also used extensively for strength and durability analysis, using the non-linear static solver. The non-linear solver uses a quasi-Newton iterative approach to solve problems in a series of load steps, conditional on achieving convergence at each step. For quasi-static problems, dynamics can be ignored, enabling predictions of structural response to large loads in a relatively small number of steps compared to an explicit solution. As the Courant condition is not applied, small elements may be used to improve accuracy without significantly increasing run times. Consequently, the non-linear implicit solver offers an effective method of quickly solving non-linear problems that require high resolution of localised stresses.

During the project, the strengths of a wide variety of components were analysed using the non-linear solver, including seat and restraint anchorages, wheelchair anchorages, exterior trim, interior systems, closures (doors, bonnet and boot lid), under a variety of loading including normal service loads and loadcases representing abusive or infrequent events.

An example is the analysis of suspension over-loading on the body structure. In these analyses a series of loadsets derived from suspension analysis were applied to the BIW model. As the cases

represent abuse conditions, small amounts of plasticity in the structure are allowable. In some cases, it was necessary to model pretension in the bolted joints, to predict joint slip. **Error! Reference source not found.** shows the example of the anti-roll bar mount, subjected to maximum loading from cross articulation of the front wheels.
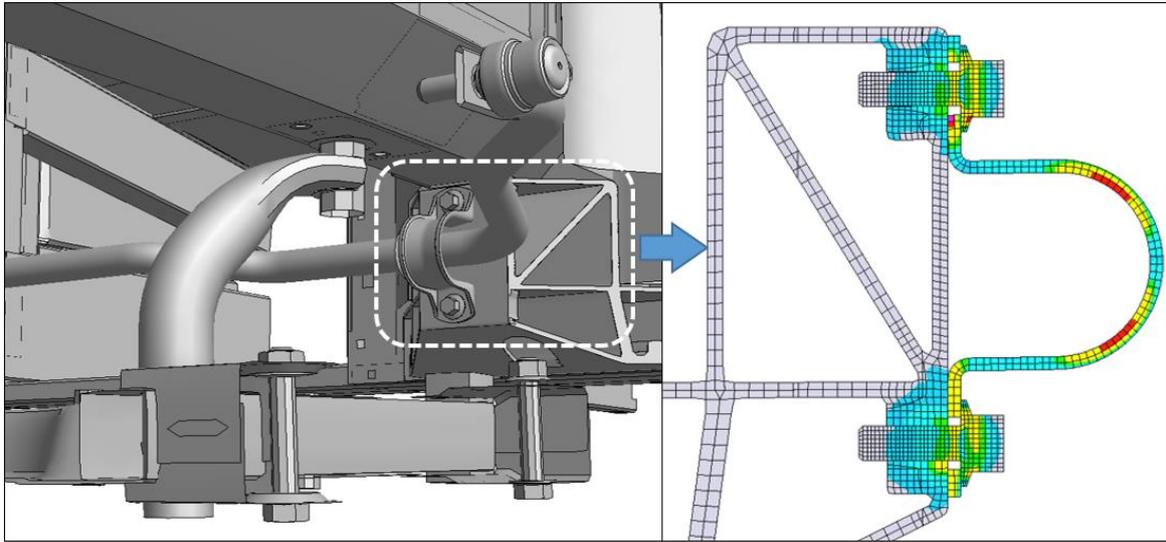

Fig.17: Detailed Model of Chassis System

Some general best-practice rules were established to ensure reliable use of the implicit solver. In each model element mesh quality was checked and any contact surface penetrations removed. Modal analysis was run to ensure that rigid body modes were not present, which would prevent a solution. Automatic timestep control was enabled to counter convergence issues during the analysis, via CONTROL_IMPLICIT_AUTO. This feature will reduce the current step size if convergence is not achieved, rather than terminating the analysis. Appropriate contact surface settings were vital for successful implicit analysis. The MORTAR contact option was found to be an effective new feature and is recommended.

6 Interiors

The modernised TX gave rise to some interesting modelling problems during the design of the interiors, many of which were unique to the design of the taxi. Of particular note were the driver's touchscreen control unit, and the divider screen between the driver and passenger compartments.
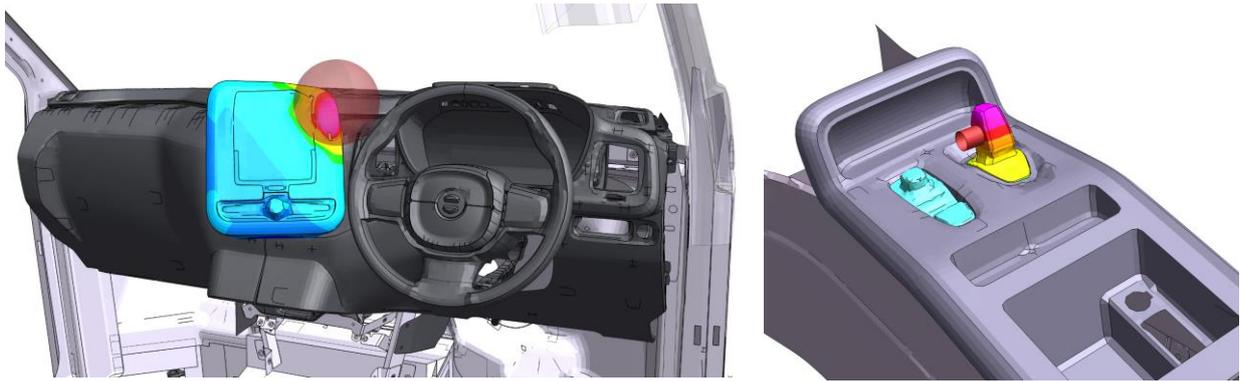
Fig.18:   *ECE R21 Interior Head Impact to the Driver's Touchscreen (left) and Abuse loading to the gear selector (right)*

It was necessary to ensure the safety of the TX's occupants for interior head impact to a number of components, such as the driver's touchscreen and the central divider, as illustrated in **Error! Reference source not found.** and **Error! Reference source not found.**. These areas were analysed in accordance to safety regulations ECE R21 and ECE R43 respectively. The touchscreen and other interior components such as the centre console and gear selector were also checked against a number of quasi-static abuse cases to ensure Emerald's stringent quality targets were met.
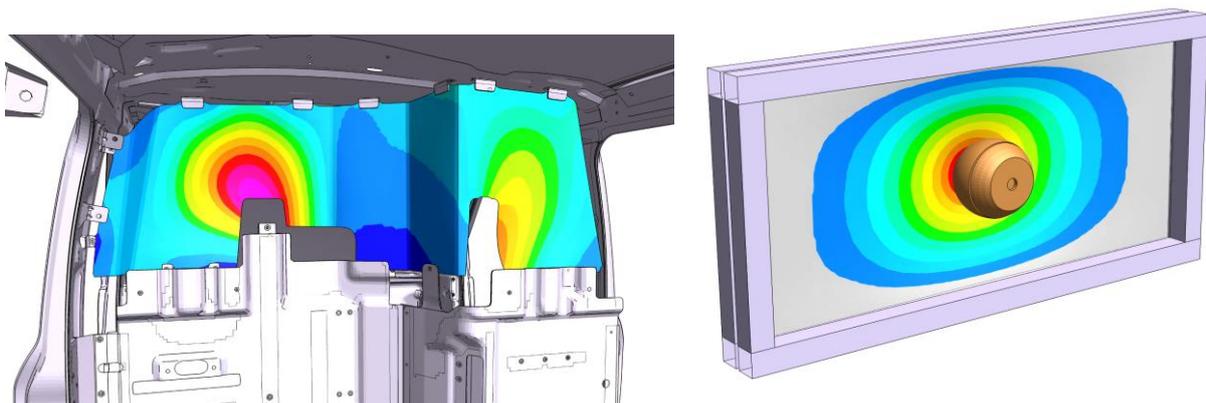

Fig.19:   *Normal Modes Analysis (left) and ECE R43 Head Impact (right) to the Central Divider*

Modal analysis of the centre divider screen and cabin space was crucial in delivering the comfortable passenger experience offered by the TX. Arup used LS-DYNA to understand the key modes of vibration of the screen with respect to the acoustic cavities, driving design changes which placed these away from key frequencies of excitation, such as from the range-extending engine.

Unlike most passenger vehicles, the front passenger compartment is designed for storing luggage rather than seating an occupant. Arup analysed a number of load cases for the trim in this area, including impact of luggage, to be sure it will stand up to the inevitable knocks and bumps during its life.
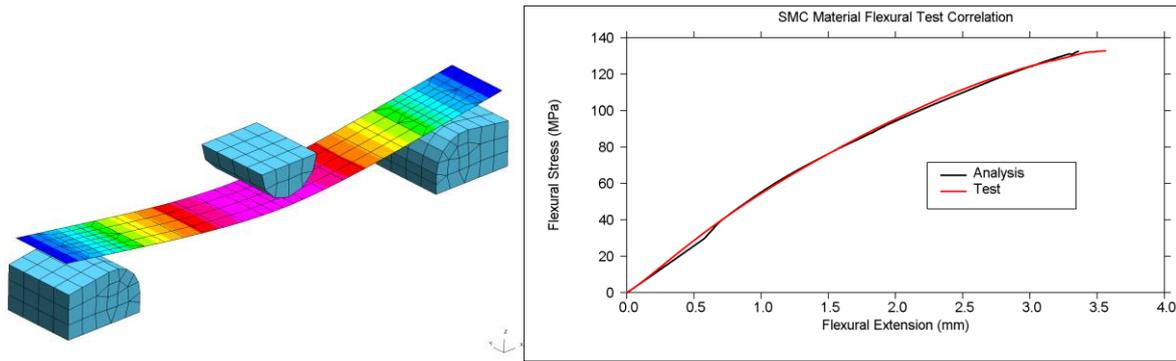
Fig.20:   SMC flexural test model (left) and correlation of flexural response to test (right)

A number of correlation exercises were performed to develop material models for the polymer components of the TX interiors and exteriors. Material model 89 (MAT_PLASTICITY_POLYMER) was found to provide a good representation of the behaviour of these materials and required only limited testing work to be performed compared to more complex material models for which the testing would have been prohibitively time consuming. MAT_PLASTICITY_POLYMER provides a simple way to model elasto-plastic materials such as polymers where the elastic and plastic regions of the stress-strain curve are not as clearly distinguishable as they are for metals, and includes strain-rate dependent response and failure [13]. **Error! Reference source not found.** presents the flexural test model used to calibrate the sheet moulded compound (SMC) material model to ISO 178 [16] and the resulting good correlation of stress against elongation up to the point of failure.

7 Closures

Analysis of the TX closures was especially efficient thanks to the use of LS-DYNA. Through careful management of the connections to the BIW, Arup were able to use the same closure include files for the full vehicle model cases as for each of the individual analyses of the TX's bonnet, front doors, rear-hinged passenger doors, and trunk lid. In each case, the full suite of strength and stiffness cases defined by EAD could be analysed by simply adding the appropriate include files containing the loads, boundary conditions, and solution controls. Further to that, as the bonnet inner geometry was being developed using the pedestrian protection analysis, the effect of the changes on overall closure performance could immediately be verified using the updated include files.

Error! Reference source not found. demonstrates this versatility being put to use; with simple selection of input files the same door model was used to model both a linear normal models analysis, and a non-linear drop-off abuse case.

Fig.21:   Rear door trimmed normal modes analysis (left) and open drop-off abuse case (right)

Error! Reference source not found. demonstrates the trunk lid being analysed for two different abuse cases; open lateral and latch loading. Use of LS-DYNA's implicit solver in analysis of the closures allowed a fast run-time whilst taking into account the non-linearities necessary for achieving an efficient design. Contact non-linearity allowed for proper interaction of the various panels, and for accurate mobilisation of the seals and bump stops, in assessment of the door window frame rigidity for example. In abuse cases, material non-linearity allowed for yielding and stress redistribution, avoiding unnecessary conservatisms.
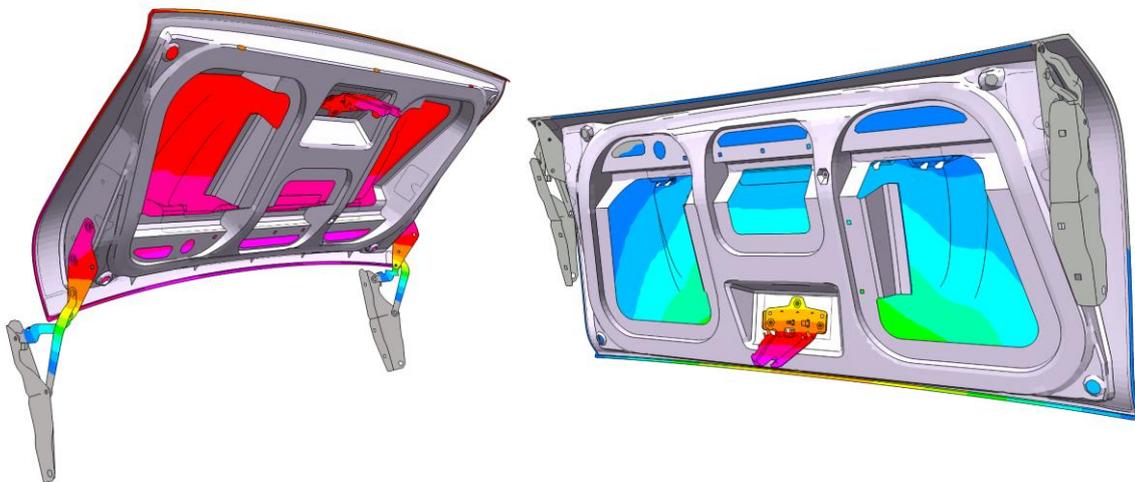

Fig.22:   Trunk Lid in Open Lateral Abuse Case (left) and Closed Latch Loading (right)

8 Pedestrian Protection

The TX was designed for the following pedestrian protection load cases in line with the requirements of the European market:

- Adult headform impact
- Child headform impact
- Flexible lower legform to bumper
- Upper legform to WAD775mm

Error! Reference source not found. presents the impact positions for the pedestrian load cases and indicates relative scorings.
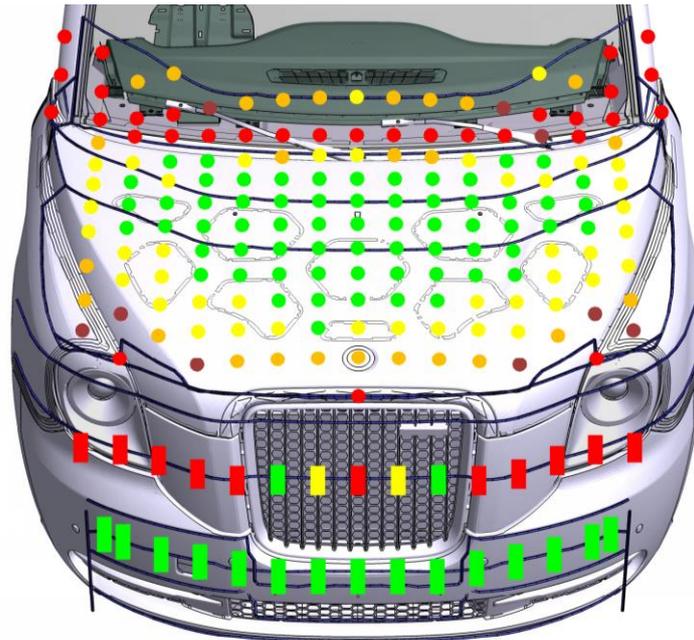

Fig.23:   Pedestrian Impact Positions and Geometry Mark-Up Lines (circle head, rectangle leg)

The LS-DYNA predictions for these load cases were critical in guiding the pedestrian protection design since prototype testing was not possible within the short development programme. The first physical testing was conducted in mid-2017, verifying the predicted performance and allowing progression directly to successful legislative sign-off testing without further design changes.

The TX was designed with a number of pedestrian protection safety features such as collapsible bonnet latch brackets and bump stops, breakable bumper fascia clips, and a specially shaped structural bumper beam with features designed to control the movement of the grille components in lower leg impact (**Error! Reference source not found.**), limiting knee ligament extensions. The form of the bonnet inner panel was developed in an analysis driven approach using the LS-DYNA head impact model. In addition to informing the shape and depth of the bonnet section, this analysis also led to the inclusion of a number of laser-cuts in the inner panel, which were shown to improve head impact criterion (HIC) values without significantly affecting bonnet strength or stiffness. Fig. 3 shows the resulting bonnet inner geometry. Forming strains from pressing analyses were included for the bonnet inner and outer panels.
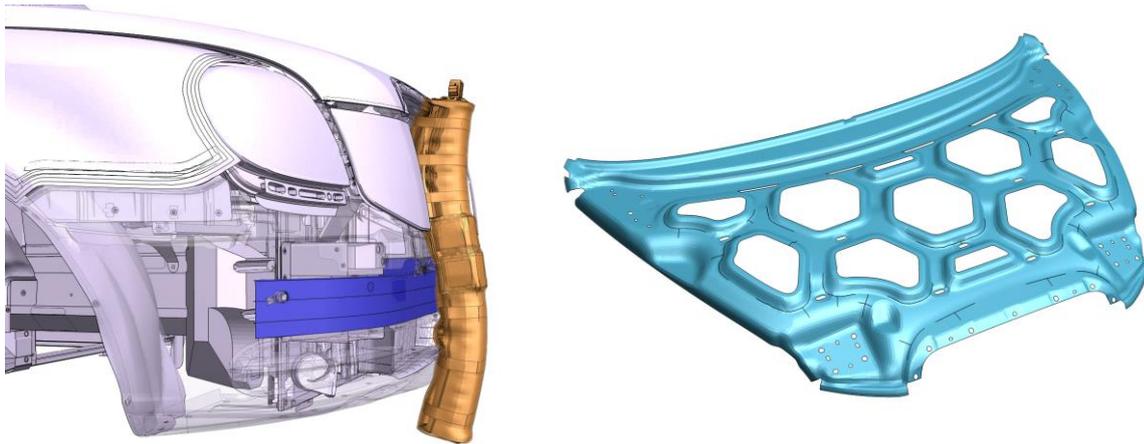
Fig.24:   Lower Legform Impact to Bumper using Humanetics Flex PLI Impactor [17], Fig. 3 - Bonnet Inner Panel Geometry with Laser Cuts

A particular challenge in the pedestrian protection design included drawing a balance between the need for a soft and energy absorbing system in the context of impact, and a stiff and robust system that met the quality and durability requirements demanded of a hard-working city taxi. This was especially true of the area near the fenders and headlamps, which predictions had shown were critical for the head impact performance. The fenders had to meet conflicting 'touch and feel' targets concerning palm-printing and dentability, whilst the headlamps had to meet strict vibration criteria. Consistent with the single-model approach discussed earlier, limited work was necessary to allow the same model to be used to assess quasi-static loading and the modal performance of these systems – ensuring the vehicle design could be considered holistically.

In addition to the analyses discussed, the LS-DYNA vehicle model was used with Oasys PRIMER's pedestrian mark-up tool to determine the targeting for each of the impactors. Through analysis of these mark-ups Arup were able to inform a number of small styling changes before running calculations that significantly improved the predicted performance; for example, reducing the extent of the child head impact zone over the headlamps and fenders.

Error! Reference source not found. demonstrates examples of the correlation achieved against test for three of the pedestrian protection injury criteria.
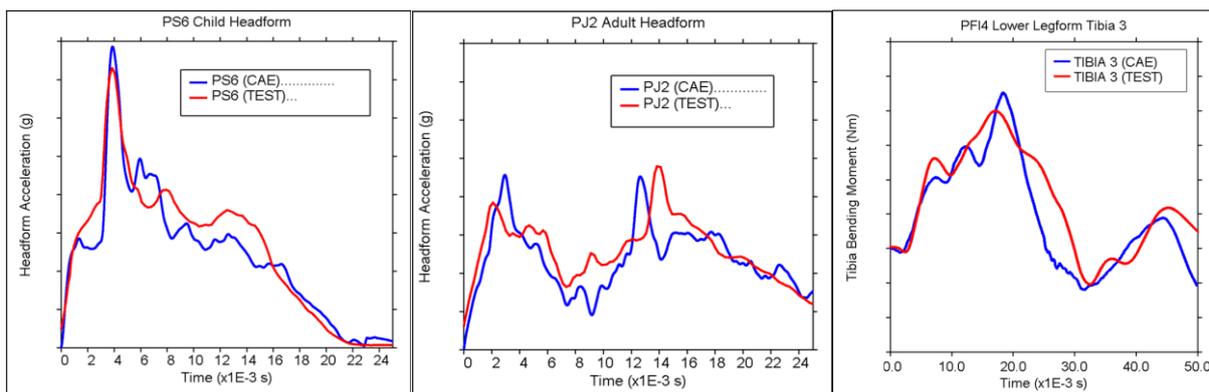

Fig.26:   CAE to Test correlation for example Child Headform (left), Adult Headform (centre) and Lower Legform (right)

9 Summary

The LEVC TX electric London taxi was released in early 2018, marking the start of a new era for the black cab. Arup supported TX designers Emerald Automotive Design (EAD) with CAE predictions using LS-DYNA. This paper has demonstrated how LS-DYNA was successfully utilised as Arup's primary analysis package across a wide variety of analysis cases. The single-model approach enabled by LS-DYNA allowed Arup to provide accurate predictions against an accelerated design program with few prototype stages.

A number of analysis methods and solution types were used with a variety of LS-DYNA's wealth of material models and keywords, leading to good correlation of predictions against physical tests. Arup's use of LS-DYNA was key in bringing this lightweight bonded aluminium taxi to market, whilst minimising energy consumption and delivering a solution to the issue of sustainable city transport.

10 References

[1]   N. Georgano and B. Munro, The London Taxi, Shire Library, 2008.

[2]   Grace's Guide, "London Electrical Cab Co," Grace's Guide to British Industrial History, 22 November 2017. [Online]. Available: https://www.gracesguide.co.uk/London_Electrical_Cab_Co. [Accessed December 2017].

[3]   (https://commons.wikimedia.org/wiki/File:1962_Austin_FX4_London_taxi.jpg), „1962 Austin FX4 London taxi", https://creativecommons.org/licenses/by-sa/3.0/legalcode.

[4]   Unisouth at English Wikipedia (https://commons.wikimedia.org/wiki/File:A_TX4_Taxi_at_Heathrow_Airport_Terminal_5.jpg), „A TX4 Taxi at Heathrow Airport Terminal 5", https://creativecommons.org/licenses/by-sa/3.0/legalcode.

[5]   LEVC, "LEVC TX - Public Affairs Strategy (Powerpoint Presentation)," London Electric Vehicle Company (LEVC), Coventry, 2017.

[6]   R. Blackden, "Black cab, U,.K. transport icon, to be made in China - Business - International Herald Tribune," The New York Times, 4 October 2006. [Online]. Available: http://www.nytimes.com/2006/10/04/business/worldbusiness/04iht-taxi.3031990.html. [Accessed December 2017].

[7]   BBC, "Manganese Bronze to call in administrators," BBC News, 22 October 2012. [Online]. Available: http://www.bbc.com/news/business-20031436. [Accessed December 2017].

[8]   BBC, "New London taxis to emit zero emissions from 2018," BBC News, 16 January 2014. [Online]. Available: http://www.bbc.com/news/uk-england-london-25756929. [Accessed December 2017].

[9]   TfL, "Taxi and Private Hire Action Plan 2016," Transport for London, September 2016. [Online]. Available: http://content.tfl.gov.uk/taxi-and-private-hire-action-plan-2016.pdf. [Accessed December 2017].

[10]   Municipality of Amsterdam, "Sustainable Amsterdam, Agenda for renewable energy, clear air, a circular economy and a climate-resilient city," March 2015. [Online]. Available: https://www.amsterdam.nl/bestuur-organisatie/organisatie/ruimte-economie/ruimte-duurzaamheid/making-amsterdam/sustainability/. [Accessed December 2017].

[11]   LEVC, TX Price and Specification Issue 1.

[12]   A. Moffat, Construction and Licensing of Motor Taxis for Use in London, Conditions of Fitness, Version 9.0, London: Transport for London (TfL), 2017.

[13]   Livermore Software Technology Corporation (LSTC), LS-DYNA Keyword User's Manual, Volume II, Material Models, 2016.

[14]   Oasys Ltd., PRIMER Version 14.0.

[15]   Livermore Software Technology Corporation (LSTC), LS-DYNA Keyword User's Manual, Volume I, 2016.

[16]   ISO 178:2010 Plastics -- Determination of Flexural Properties, International Organisation for Standardization (ISO), 2012.

[17]   Humantics, FLEX PLI GTR REGULATED V1.0.1 LS-DYNA Model, Plymouth, Michigan, USA: Humanetics Innovative Solutions, Inc., August 2016.